IPEM
Institute of Physics and Engineering in Medicine

Three-dimensional image reconstruction from complete projections

To cite this article: M Defrise *et al* 1989 *Phys. Med. Biol.* **34** 573

Phys. Med. Biol., 1989, Vol. 34, No 5, 573-587. Printed in the UK

Three-dimensional image reconstruction from complete projections

M Defrise†, D W Townsend‡ and R Clack§

† Division of Nuclear Medicine, Akademisch Ziekenhuis VUB, Brussels, Belgium
‡ Division of Nuclear Medicine, Geneva University Hospital, Geneva, Switzerland
§ Department of Mathematics, Dalhousie University, Halifax, Canada

Received 5 October 1988

Abstract. Three-dimensional medical image reconstruction for both transmission and emission tomography has traditionally decomposed the problem into a set of two-dimensional reconstructions on parallel transverse sections. There is, however, increasing interest in reconstructing projection data directly in three dimensions. For emission tomography in particular, such a reconstruction procedure would clearly make more efficient use of the available photon flux. In the past few years, a number of authors have studied the problems associated with full three-dimensional reconstruction, especially in the case of positron tomography where three-dimensional reconstruction is likely to offer the greatest benefits. While most approaches follow that of filtered backprojection, the relationship between the various filters that have been proposed is far from evident. This paper clarifies this relationship by analysing and generalising the different classes of published filters and establishes the properties and characteristics of a general solution to the three-dimensional reconstruction problem. Some guidelines are suggested for the choice of an appropriate filter in a given situation.

1. Introduction

The traditional approach to three-dimensional medical image reconstruction for both transmission and emission tomography decomposes the problem into a set of two-dimensional reconstructions on independent parallel sections. Each two-dimensional section is reconstructed from a set of one-dimensional projection data using a standard filtered backprojection algorithm (Herman 1980, Barrett and Swindell 1981, Natterer 1986). However, while this approach is computationally efficient, photons which pass obliquely through the chosen set of sections cannot be included in the reconstruction. This is a particular disadvantage in emission tomography where the photons are emitted isotropically and only a fraction of the available flux is actually used in the reconstruction. In transmission tomography, collimation of the x-ray source to emit within a transverse plane prevents exposure of the patient to unnecessary radiation. In emission tomography, since the source cannot be collimated, it is usual to shield the detector in order to eliminate oblique rays. This shielding also serves to reduce both the total incident photon flux and the fraction of scattered photons.

It is evident that, in emission tomography, more efficient usage would be made of the emitted photons if the oblique rays were also included in the reconstruction. To achieve this goal, the detector must be operated without shielding and a fully three-dimensional reconstruction algorithm used to process the data. Although this idea is not new, applications in medical imaging remain marginal because of a number of technical and computational difficulties. Removal of the collimation, while permitting the detection of oblique rays, also increases the sensitivity of the system to scattered photons and other sources of contrast-reducing background. Furthermore, conventional two-dimensional reconstruction techniques cannot be straightforwardly generalised to three dimensions, with one exception in the case of full 4π angular acceptance, which necessitates an impractical spherical detector geometry. Three-dimensional reconstructions generally impose a heavy computational load on the data processing.

In medical imaging, three-dimensional reconstruction incorporating oblique rays has been studied mainly for cone beam transmission tomography and for positron emission tomography. The two applications lead to rather different reconstruction problems owing to fundamental differences in the input data sets. Cone beam tomography requires inversion of the divergent beam transform since the integrals of density are measured along straight lines radiating from the position of the x-ray source. Details of this problem and its solution have been published by Smith (1985), Natterer (1986) and Grangeat (1987), and cone beam geometry will not be considered further in this paper.

In positron emission tomography (PET), three-dimensional reconstruction algorithms were developed originally for stationary, planar, position-sensitive detectors (Chu and Tam 1977, Schorr and Townsend 1981) and more recently for rotating planar detectors (Colsher 1980, Schorr *et al* 1983) and stationary truncated spherical detector arrays (Ra *et al* 1982). Three-dimensional reconstruction algorithms attempt to recover the distribution of a positron-emitting isotope from a set of two-dimensional projections. This recovery procedure is not unique; a number of distinct algorithms are available which do not produce the same reconstructed image when the projection data contain noise. These differences are fundamental and do not originate only from the discretisation or implementation procedure. The reason for this non-uniqueness lies in a redundancy of the three-dimensional data. While lines in two dimensions (2D) are specified by two parameters (slope and intercept) and are used to reconstruct a density function which depends on two spatial variables (x, y), lines in three dimensions (3D) require four parameters (two slopes and two intercepts) and are used to reconstruct a density function which depends on three spatial variables (x, y, z). The inversion procedure is therefore overdetermined, as was originally noted by Orlov (1976) in his seminal work on three-dimensional reconstruction for x-ray crystallography, and more recently by Pelc and Chesler (1979).

The aims of this paper are to clarify the relationship between the different published algorithms, to establish the properties and characteristics of a general solution and to indicate guidelines for the choice of an appropriate filter. The paper will focus on algorithms based on a shift-invariant system response. Shift invariance requires that, if one line integral is measured in a particular direction, all line integrals are measured in that direction through all points within the field of view, i.e. all projections in the data set must be complete. An equation for the general linear shift-invariant inversion formula will be given. The equation will be investigated separately for two different classes of reconstruction filters: factorisable and non-factorisable. In this context, a factorisable filter is one for which the frequency space representation can be separated into the product of the angular component for the projection direction and a component which depends upon the frequency space coordinates within the projection. As will be seen, a direct consequence of this separability is that the operations of filtering and backprojection can be interchanged. An optimal property of factorisable filters will be established that could help in selecting the most appropriate filter to use in practice.

The treatment throughout this paper will be mainly theoretical; problems concerned with the discretisation or computer implementation aspects of the algorithms will not be discussed.

2. The general condition for the recovery filter

The line integrals $p(\hat{\boldsymbol{u}}, \boldsymbol{s})$ of a density $f(\boldsymbol{x})$ measured for a set of directions Ω are defined by

$$p(\hat{\boldsymbol{u}}, \boldsymbol{s}) = \int_{-\infty}^{+\infty} \mathrm{d}l\, f(\boldsymbol{s} + l\hat{\boldsymbol{u}}) \tag{1}$$

where $\hat{\boldsymbol{u}}$ is a unit vector with $\hat{\boldsymbol{u}} \in \Omega$ and $\boldsymbol{s} \,.\, \hat{\boldsymbol{u}} = 0$. The aperture Ω is assumed to be shift invariant, so that for each direction $\hat{\boldsymbol{u}} \in \Omega$ the line integrals are measured for all positions in the central plane normal to $\hat{\boldsymbol{u}}$, i.e. for all $\boldsymbol{s} \in R^3$ satisfying $\boldsymbol{s} \,.\, \hat{\boldsymbol{u}} = 0$. For simplicity, Ω is taken to be symmetrical with respect to the origin (if $\hat{\boldsymbol{u}} \in \Omega$ then $-\hat{\boldsymbol{u}} \in \Omega$), and the projection is an even function on $\Omega(p(\hat{\boldsymbol{u}}, \boldsymbol{s}) = p(-\hat{\boldsymbol{u}}, \boldsymbol{s}))$.

The relationship (1) between the density f and the projections p is expressed in Fourier space by the central slice theorem (Natterer 1986 p11)

$$F(\boldsymbol{\nu}) = \iiint_{R^3} \mathrm{d}^3x\, f(\boldsymbol{x}) \exp(-2\pi \mathrm{i} \boldsymbol{x} \cdot \boldsymbol{\nu}) = P(\hat{\boldsymbol{u}}, \boldsymbol{\nu}) \tag{2}$$

with $\hat{\boldsymbol{u}} \cdot \boldsymbol{\nu} = 0$. $P(\hat{\boldsymbol{u}}, \boldsymbol{\nu})$ is the two-dimensional Fourier transform of the projection

$$P(\hat{\boldsymbol{u}}, \boldsymbol{\nu}) = \iint_{\boldsymbol{s}.\hat{\boldsymbol{u}}=0} \mathrm{d}^2 s \exp(-2\pi \mathrm{i} \boldsymbol{s} \cdot \boldsymbol{\nu}) p(\hat{\boldsymbol{u}}, \boldsymbol{s}) \qquad \hat{\boldsymbol{u}} \cdot \boldsymbol{\nu} = 0. \tag{3}$$

A given projection $p(\hat{\boldsymbol{u}}, \boldsymbol{s})$, for all $\boldsymbol{s}$, therefore samples the Fourier transform $F(\boldsymbol{\nu})$ of $f(\boldsymbol{x})$ on the frequency plane through the origin (a *central* plane) and normal to the unit vector $\hat{\boldsymbol{u}}$. A set of projections thus samples $f(\boldsymbol{x})$ on a corresponding set of central planes in frequency space. Since, in general, some of these planes will intersect, a given frequency component $F(\boldsymbol{\nu})$ may be sampled by more than one projection, a situation which, in two dimensions, arises only at the origin. This shows that a necessary and sufficient condition for the existence of a unique solution to the inversion of equation (1) is that, for any frequency $\boldsymbol{\nu}$, at least one projection must be available which satisfies $\hat{\boldsymbol{u}} \cdot \boldsymbol{\nu} = 0$ in order to recover $F(\boldsymbol{\nu})$ using the central slice theorem. Geometrically, this condition (Orlov 1976) requires that the aperture region Ω should intersect all equatorial circles on the unit sphere. However, even if Orlov's condition is not satisfied, the solution may still be unique provided that the set of admissible solutions is further restricted, e.g. from knowledge of the bounded support of the function $f(\boldsymbol{x})$. In this case, the inversion problem is severely ill-posed (Tam and Perez-Mendez 1981a, b), a situation similar to the limited-angle tomography problem in 2D (Davison 1983). Throughout this paper it will be assumed that Orlov's condition is satisfied.

The most general linear and shift-invariant inversion formula for equation (1) can be shown to be a filtered backprojection

$$f(\boldsymbol{x}) = \iint_{\Omega} \mathrm{d}^2\hat{\boldsymbol{u}}\, p^{\mathrm{F}}[\hat{\boldsymbol{u}}, \boldsymbol{x} - (\boldsymbol{x}\,.\,\hat{\boldsymbol{u}})\hat{\boldsymbol{u}}] \tag{4}$$

where $\boldsymbol{x} - (\boldsymbol{x} \cdot \hat{\boldsymbol{u}})\hat{\boldsymbol{u}}$ is the projection of the vector $\boldsymbol{x}$ onto the plane normal to the unit vector $\hat{\boldsymbol{u}}$, and the filtered projections p^{F} are obtained from a 2D convolution with a kernel h (defined as a generalised function) by

$$p^{\mathrm{F}}(\hat{\boldsymbol{u}}, \boldsymbol{s}) = \iint_{\boldsymbol{s}'.\hat{\boldsymbol{u}}=0} \mathrm{d}^2 s'\, h(\hat{\boldsymbol{u}}, \boldsymbol{s} - \boldsymbol{s}')p(\hat{\boldsymbol{u}}, \boldsymbol{s}') \qquad \boldsymbol{s} \cdot \hat{\boldsymbol{u}} = 0. \tag{5}$$

Taking the Fourier transform of both sides of equation (5) gives

$$P^{\mathrm{F}}(\hat{\boldsymbol{u}}, \boldsymbol{\nu}) = P(\hat{\boldsymbol{u}}, \boldsymbol{\nu})H(\hat{\boldsymbol{u}}, \boldsymbol{\nu}) \qquad \hat{\boldsymbol{u}} \cdot \boldsymbol{\nu} = 0 \tag{6}$$

where the upper case characters denote 2D Fourier transforms, defined as in equation (3). The projections $p(\hat{\boldsymbol{u}}, \boldsymbol{s})$ may therefore be equivalently filtered in Fourier space according to equation (6).

A number of specific Fourier space filters $H(\hat{\boldsymbol{u}}, \boldsymbol{\nu})$ have been described in the literature (Colsher 1980, Schorr *et al* 1983, Ra *et al* 1982) which permit the exact reconstruction of any density $f(\boldsymbol{x})$. It is useful to derive an equation which must be satisfied by any valid reconstruction filter. Specific filters can then be shown to be particular solutions of this equation (cf. §§ 3 and 4).

Taking the Fourier transform of both sides of equation (4), and using equation (5) and the representation of the Dirac distribution as

$$\delta(x) = \lim_{b \to \infty} \int_{-b}^{b} \mathrm{d}y \exp(-2\pi \mathrm{i} xy) \tag{7}$$

results in

$$F(\boldsymbol{\nu}) = \iint_{\Omega} \mathrm{d}^2\hat{\boldsymbol{u}}\, \delta(\hat{\boldsymbol{u}} \cdot \boldsymbol{\nu})H(\hat{\boldsymbol{u}}, \boldsymbol{\nu})P(\hat{\boldsymbol{u}}, \boldsymbol{\nu}). \tag{8}$$

Using the central slice theorem (2) we now replace $P(\hat{\boldsymbol{u}}, \boldsymbol{\nu})$ by $F(\boldsymbol{\nu})$ in equation (8). Since the resulting equation must be satisfied for any density $f(\boldsymbol{x})$, it follows that any valid filter function $H(\hat{\boldsymbol{u}}, \boldsymbol{\nu})$ must satisfy

$$\iint_{\Omega} \mathrm{d}^2\hat{\boldsymbol{u}}\, \delta(\hat{\boldsymbol{u}} \cdot \boldsymbol{\nu})H(\hat{\boldsymbol{u}}, \boldsymbol{\nu}) = 1 \tag{9}$$

for any $\boldsymbol{\nu}$ in R^3.

As will be seen, an infinite number of filters can be derived which satisfy the necessary and sufficient condition (9). These filters are not, however, equivalent in that they do not yield identical reconstructions unless the data are consistent, i.e. belong to the range of the x-ray transform given by equation (1). This is, in general, only true if the data are noise free, and therefore in practice the various filters differ in the way in which they propagate noise. Discretisation and numerical implementation may, of course, introduce further differences between mathematically equivalent algorithms, a situation which is well known in 2D tomography.

This paper will examine two families of filters satisfying equation (9): those which are factorisable and those which are not factorisable.

3. Factorisable filters

A filter is said to be factorisable if it can be written as the product of a filter function $H'(\boldsymbol{\nu})$ defined on R^3, with an even positive integrable function $w(\hat{\boldsymbol{u}})$ defined on Ω:

$$H(\hat{\boldsymbol{u}}, \boldsymbol{\nu}) = H'(\boldsymbol{\nu}) w(\hat{\boldsymbol{u}}) \qquad \boldsymbol{\nu} \cdot \hat{\boldsymbol{u}} = 0. \tag{10}$$

Geometrically this means that each projection $p(\hat{\boldsymbol{u}}, \boldsymbol{\nu})$ is filtered using a filter $H(\hat{\boldsymbol{u}}, \boldsymbol{\nu})$ which is proportional to the central section normal to $\hat{\boldsymbol{u}}$ through a 3D filter function $H'(\boldsymbol{\nu})$. A factorisable filter can be constructed for any positive function $w(\hat{\boldsymbol{u}})$; indeed, when $w(\hat{\boldsymbol{u}})$ is given, equation (9) uniquely determines the filter from

$$H'(\boldsymbol{\nu}) = \frac{1}{\iint_\Omega \mathrm{d}^2\hat{\boldsymbol{u}}\, w(\hat{\boldsymbol{u}})\, \delta(\hat{\boldsymbol{u}} \cdot \boldsymbol{\nu})}. \tag{11}$$

This family (for different $w(\hat{\boldsymbol{u}})$) of reconstruction filters was first derived by Schorr *et al* (1983). The inversion formula of Orlov (1976) belongs to this family. As was shown by Kinahan *et al* (1987), Orlov's formula is equivalent to filtered backprojection with the filter derived by Colsher (1980) for the particular case of a truncated cylindrical detector with $w(\hat{\boldsymbol{u}}) = 1$. Indeed most of the published truly 3D reconstruction algorithms involve factorisable filters.

Factorisable filters have a number of interesting properties, the practical implications of which will be discussed below.

3.1. Commuting the filtering and backprojection operations

The filtering and backprojection operations of the inversion procedure given by equations (4) and (5) can be commuted for factorisable filters. Therefore, it is possible to perform an equivalent inversion by backprojecting prior to filtering, in analogy with the so-called 'rho-filtered layergram' approach in 2D (Smith *et al* 1973). Thus from equations (8) and (10)

$$f(\boldsymbol{x}) = \iiint \mathrm{d}^3 y\, h'(\boldsymbol{x} - \boldsymbol{y}) b_\Omega(\boldsymbol{y}) \tag{12}$$

where the generalised function $h'(\boldsymbol{x})$ is the inverse 3D Fourier transform of the filter $H'(\boldsymbol{\nu})$ and the backprojected distribution $b_\Omega(\boldsymbol{x})$ is defined as

$$b_\Omega(\boldsymbol{x}) = \iint_\Omega \mathrm{d}^2\hat{\boldsymbol{u}}\, w(\hat{\boldsymbol{u}}) p[\hat{\boldsymbol{u}}, \boldsymbol{x} - (\boldsymbol{x} \cdot \hat{\boldsymbol{u}})\hat{\boldsymbol{u}}] \tag{13}$$

which is the 3D inverse Fourier transform of

$$\iint_\Omega \mathrm{d}^2\hat{\boldsymbol{u}}\, \delta(\hat{\boldsymbol{u}} \cdot \boldsymbol{\nu}) w(\hat{\boldsymbol{u}}) P(\hat{\boldsymbol{u}}, \boldsymbol{\nu}).$$

The backprojection of a point source at the origin, $\delta^3(\boldsymbol{x})$, is usually known as the point response function (PRF) of the system. From equation (13)

$$\begin{aligned}\mathrm{PRF}(\boldsymbol{x}) &= \iint_\Omega \mathrm{d}^2\hat{\boldsymbol{u}}\, w(\hat{\boldsymbol{u}})\, \delta^2[\boldsymbol{x}-(\boldsymbol{x}\cdot\hat{\boldsymbol{u}})\hat{\boldsymbol{u}}] \\ &= \frac{2}{|\boldsymbol{x}|^2} w\left(\frac{\boldsymbol{x}}{|\boldsymbol{x}|}\right) \qquad \text{if } \frac{\boldsymbol{x}}{|\boldsymbol{x}|}\in\Omega \\ &= 0 \qquad\qquad\qquad\quad \text{otherwise.}\end{aligned} \tag{14}$$

Taking the Fourier transforms of both sides of equation (14) and comparing with equation (11), it can be seen that the 3D filter $H'(\boldsymbol{\nu})$ is the reciprocal of the Fourier transform of the PRF.

The factorisability of the filter $H(\hat{\boldsymbol{u}}, \boldsymbol{\nu})$ is an essential requirement in order to derive equations (12) and (13). In general, in 3D, the dependence of the filter on $\hat{\boldsymbol{u}}$ and $\boldsymbol{\nu}$ cannot be separated in this way and therefore there is no equivalent form of the rho-filtered layergram for non-factorisable filters. Nevertheless, the possibility to perform the backprojection operation before filtering can be important for certain applications, particularly in 3D, where the number of sampled projections can be very large. The essential advantage of backprojection before filtering arises from the fact that the sorting of the data into explicit projections can be avoided. In positron tomography, each projection value represents the sum of a number of individual coincidence events and, from the linearity of the backprojection process, these events may be backprojected one at a time, thereby avoiding the sorting into projections. For this procedure to yield a valid reconstruction, the corresponding filter must be factorisable.

3.2. *The filter H' is proportional to the modulus of the frequency, $|\boldsymbol{\nu}|$*

Equation (11) can be rewritten as

$$H'(\boldsymbol{\nu}) = |\boldsymbol{\nu}| \frac{1}{\iint_\Omega \mathrm{d}^2\hat{\boldsymbol{u}}\, w(\hat{\boldsymbol{u}})\, \delta(\hat{\boldsymbol{u}}\cdot\boldsymbol{\nu}/|\boldsymbol{\nu}|)} \tag{15}$$

where the denominator depends only on the direction of the frequency $\boldsymbol{\nu}$ (Schorr *et al* 1983). The frequency dependence of the 3D factorisable filter is thus the same as that of the standard ramp filter in two dimensions, which reflects the same mildly ill-posed nature of the inversion problem associated with this ramp-like behaviour. The usual apodising windows (e.g. a Hanning window) can be used to regularise the reconstruction.

3.3. *Optimality of the factorisable filters*

A possible criterion for selecting a filter which satisfies equation (9) is to choose the one which minimises the variance in the reconstructed image. Assume first that all projections $p(\hat{\boldsymbol{u}}, s)$ have been measured with the same accuracy and evaluate $F(\boldsymbol{\nu})$ from $P(\hat{\boldsymbol{u}}, \boldsymbol{\nu})$ according to the equation (8), which can be interpreted as a weighted average of all available estimates of a given Fourier component $F(\boldsymbol{\nu})$. Then the variance of $F(\boldsymbol{\nu})$ will be minimum if all contributions to the average are equally weighted, i.e. if $H(\hat{\boldsymbol{u}}, \boldsymbol{\nu})$ is independent of $\hat{\boldsymbol{u}}$. Such a requirement is obviously satisfied by a factorisable filter with $w(\hat{\boldsymbol{u}})=1$. This heuristic argument can be expressed more rigorously by introducing the following mathematical property.

Let $w(\hat{\boldsymbol{u}})$ be some fixed positive integrable function on Ω. Among all filters $H(\hat{\boldsymbol{u}}, \boldsymbol{\nu})$ satisfying the general condition, equation (9), the factorisable filter, equation (10), minimises the quantity

$$v(H, \boldsymbol{\nu})=\iint_{\Omega} \mathrm{d}^2\hat{\boldsymbol{u}}\, \delta(\hat{\boldsymbol{u}}\cdot\boldsymbol{\nu}) \frac{1}{w(\hat{\boldsymbol{u}})}|H(\hat{\boldsymbol{u}}, \boldsymbol{\nu})|^2 \tag{16}$$

for any fixed frequency $\boldsymbol{\nu}$.

This can be seen from the following inequality:

$$\begin{aligned} 0 &\leqslant \iint_{\Omega} \mathrm{d}^2\hat{\boldsymbol{u}}\, \delta(\hat{\boldsymbol{u}}\cdot\boldsymbol{\nu}) \frac{1}{w(\hat{\boldsymbol{u}})}|H(\hat{\boldsymbol{u}}, \boldsymbol{\nu})-w(\hat{\boldsymbol{u}})H'(\boldsymbol{\nu})|^2 \\ &= v(H, \boldsymbol{\nu})+v(wH', \boldsymbol{\nu})-2H'(\boldsymbol{\nu}) = v(H, \boldsymbol{\nu})-v(wH', \boldsymbol{\nu}) \end{aligned} \tag{17}$$

with $v(H, \boldsymbol{\nu})$ given by equation (16) and H' given by equation (11).

The interpretation of this result is as follows. Consider the measured line integrals $p(\hat{\boldsymbol{u}}_i, \boldsymbol{s}_j)$ as independent random variables with variance (due to measurement errors) $\sigma^2(\hat{\boldsymbol{u}}_i, \boldsymbol{s}_j)$. Assuming that the projection sampling is sufficiently fine and uniform, the density function $f(\boldsymbol{x})$ can be reconstructed by discretising the filtered backprojection formula given by equations (4) and (5):

$$f(\boldsymbol{x}) \approx \Delta_u\Delta_s \sum_i \sum_j h_S[\hat{\boldsymbol{u}}_i, \boldsymbol{x}-(\boldsymbol{x}\cdot\hat{\boldsymbol{u}}_i)\hat{\boldsymbol{u}}_i-\boldsymbol{s}_j]\, p(\hat{\boldsymbol{u}}_i, \boldsymbol{s}_j) \tag{18}$$

where Δ_u and Δ_s are quadrature weights (assuming uniform sampling), and h_S is a reconstruction kernel, apodised using some appropriate smoothing filter $S(\boldsymbol{\nu})$, i.e. its Fourier transform is given by

$$H_S(\hat{\boldsymbol{u}}, \boldsymbol{\nu}) = H(\hat{\boldsymbol{u}}, \boldsymbol{\nu})S(\boldsymbol{\nu}) \tag{19}$$

for some filter $H(\hat{\boldsymbol{u}}, \boldsymbol{\nu})$ satisfying equation (9). The variance of the image estimate (18) at $\boldsymbol{x}$ is

$$\mathrm{var}\{f(\boldsymbol{x})\} = \Delta_u^2\Delta_s^2 \sum_i \sum_j h_S^2[\hat{\boldsymbol{u}}_i, \boldsymbol{x}-(\boldsymbol{x}\cdot\hat{\boldsymbol{u}}_i)\hat{\boldsymbol{u}}_i-\boldsymbol{s}_j]\,\sigma^2(\hat{\boldsymbol{u}}_i, \boldsymbol{s}_j). \tag{20}$$

Using the fact that the discrete summations approximate the double integral over $\hat{\boldsymbol{u}}$ and $\boldsymbol{s}$, this can be rewritten as

$$\mathrm{var}\{f(\boldsymbol{x})\} \approx \Delta_u\Delta_s \iint_{\Omega} \mathrm{d}^2\hat{\boldsymbol{u}} \iint_{\hat{\boldsymbol{u}}.\boldsymbol{s}=0} \mathrm{d}^2\boldsymbol{s}\, h_S^2(\hat{\boldsymbol{u}}, \boldsymbol{s})\,\sigma^2[\hat{\boldsymbol{u}}, \boldsymbol{x}-(\boldsymbol{x}\cdot\hat{\boldsymbol{u}})\hat{\boldsymbol{u}}-\boldsymbol{s}] \tag{21}$$

where $\sigma^2(\hat{\boldsymbol{u}}, \boldsymbol{s})$ is a function interpolating the measurement variances $\sigma^2(\hat{\boldsymbol{u}}_i, \boldsymbol{s}_j)$. The square of the kernel h_S is a sharply peaked function around $\boldsymbol{s}=0$, whereas, except near boundaries, $\sigma^2(\hat{\boldsymbol{u}}, \boldsymbol{s})$ is assumed to vary only slowly with $\boldsymbol{s}$. We therefore approximate $\boldsymbol{s}$ by $\mathbf{0}$ in the argument of σ^2. Using Parseval's relation

$$\iint_{\hat{\boldsymbol{u}}.\boldsymbol{s}=0} \mathrm{d}^2\boldsymbol{s}\, h_S^2(\hat{\boldsymbol{u}}, \boldsymbol{s}) = \iint_{\hat{\boldsymbol{u}}.\boldsymbol{\nu}=0} \mathrm{d}^2\boldsymbol{\nu}\, |H(\hat{\boldsymbol{u}}, \boldsymbol{\nu})|^2 S^2(\boldsymbol{\nu}) \tag{22}$$

we finally obtain for the image variance at x

$$\mathrm{var}\{f(x)\} \approx \Delta_u \Delta_s \iint\limits_{\Omega} \mathrm{d}^2\hat{u}\, \sigma^2[\hat{u}, x - (x \cdot \hat{u})\hat{u}] \iint\limits_{\hat{u}.\nu=0} \mathrm{d}^2\nu\, |H(\hat{u}, \nu)|^2 S^2(\nu). \tag{23}$$

Thus the extremum property (16), being valid for any ν, implies that the factorisable filter given by equation (11) with $w(\hat{u}) = 1/\sigma^2[\hat{u}, x - (x \cdot \hat{u})\hat{u}]$ minimises the variance of the reconstructed density $f(x)$ at x. Likewise, the variance integrated over a bounded region D is minimised by taking

$$w(\hat{u}) = \frac{1}{\iiint_D \mathrm{d}^3x\, \sigma^2[\hat{u}, x - (x \cdot \hat{u})\hat{u}]} \tag{24}$$

4. Non-factorisable filters

A valid reconstruction filter satisfying equation (9) need not be factorisable in the form of equation (10) and as discussed in § 3. Indeed, as shown in the Appendix, non-factorisable filters can be constructed for any non-trivial aperture Ω. Sections 4.1 and 4.2 focus on one particular family of non-factorisable filters, an example of which was introduced originally by Ra *et al* (1982) for a truncated spherical detector. A slightly more general form of this filter will be derived in order to clarify the relationship, and emphasise the differences, between the factorisable filters and this alternative family of solutions to equation (9). For the particular case of a truncated cylindrical detector, the explicit form of the factorisable filter proposed by Colsher (1980) will be compared with the non-factorisable filter of Ra *et al* (1982) in order to clarify the significance of the optimality property described in § 3. Finally, in § 4.3, a family of recovery filters will be derived for this geometry, thus providing a clear illustration of the redundancy in the 3D data set.

4.1. The TTR algorithm

Ra *et al* (1982) observed that a 3D image may be considered as a series of independent 2D slices. In conventional 2D tomography, as mentioned in the Introduction, reconstruction is restricted to a set of non-intersecting slices by eliminating oblique rays. However, in principle, the same 2D algorithms can be used to reconstruct any slice, including oblique slices, provided that the data set includes all the line integrals of the density function required for such a reconstruction. The slices, or planes, that contain such a completely measured set of line integrals are here referred to as *valid* planes, and they will be identified by their unit normal vector $\hat{o}$. The set of orientation vectors $\hat{o}$ of all valid planes containing the point x is denoted as $A(x)$:

$$A(x) = \{\hat{o} \in S^2 | \, p(\hat{u}, s) \text{ is measured for all } \hat{u}, s \text{ such that } \hat{u} \cdot \hat{o} = 0 \text{ and } s \cdot \hat{o} = x \cdot \hat{o}\}. \tag{25}$$

Since the aperture Ω is shift invariant, if one plane normal to a given orientation vector $\hat{o}$ is valid, then the whole set of parallel planes is valid. The set of valid orientation vectors can be written as

$$A(x) = A = \left\{ \hat{o} \in S^2 \,\middle|\, \iint\limits_{\Omega} \mathrm{d}^2\hat{u}\, \delta(\hat{u} \cdot \hat{o}) = 2\pi \right\} \tag{26}$$

i.e. the whole equatorial circle normal to $\hat{\boldsymbol{o}}$ must be contained within Ω, which is simply the usual requirement for a 2D reconstruction. It should be noted that in 3D the set of valid planes A may still be empty even when Ω satisfies Orlov's condition, although this would only occur for rather unrealistic detector geometries. Consider for instance an aperture Ω built as the union of two non-adjacent sets Ω_1 and Ω_2 on the unit sphere, neither of which separately satisfies Orlov's condition but chosen in such a way that any equatorial circle intersects either Ω_1 or Ω_2 (or both). The aperture Ω satisfies Orlov's condition but no equatorial circle can be entirely contained in Ω, so that A is empty. Therefore the TTR (truly three-dimensional) algorithm described hereafter cannot be applied in this case.

A given point $\boldsymbol{x}$ in the field of view will lie on a number of valid planes and, therefore, it is natural to reconstruct the density function f at $\boldsymbol{x}$ as a weighted average of all 2D reconstructions of planes through $\boldsymbol{x}$. Thus

$$f(\boldsymbol{x}) = \frac{1}{\iint_A \mathrm{d}^2\hat{\boldsymbol{o}}\, w(\hat{\boldsymbol{o}})} \iint_A \mathrm{d}^2\hat{\boldsymbol{o}}\, w(\hat{\boldsymbol{o}}) f(\boldsymbol{x}, \hat{\boldsymbol{o}}) \tag{27}$$

where $w(\hat{\boldsymbol{o}})$ is a positive even integrable function and the 2D reconstruction $f(\boldsymbol{x}, \hat{\boldsymbol{o}})$ of $f(\boldsymbol{x})$ in the plane orthogonal to $\hat{\boldsymbol{o}}$ through $\boldsymbol{x}$ is obtained using a 2D filtered back-projection:

$$f(\boldsymbol{x}, \hat{\boldsymbol{o}}) = \iint_\Omega \mathrm{d}^2\hat{\boldsymbol{u}}\, \delta(\hat{\boldsymbol{o}} . \hat{\boldsymbol{u}}) p^{\mathrm{F}}[\hat{\boldsymbol{u}}, \boldsymbol{x} - (\boldsymbol{x} \cdot \hat{\boldsymbol{u}})\hat{\boldsymbol{u}}]. \tag{28}$$

The double integral over $\hat{\boldsymbol{u}}$ corresponds to a backprojection in the plane normal to $\hat{\boldsymbol{o}}$, and p^{F} is obtained by a one-dimensional (1D) convolution of the projections:

$$p^{\mathrm{F}}(\hat{\boldsymbol{u}}, \boldsymbol{s}) = \iint_{\hat{\boldsymbol{u}}.\boldsymbol{s}'=0} \mathrm{d}^2\boldsymbol{s}'\, \delta(\boldsymbol{s}' \cdot \hat{\boldsymbol{o}}) k(|\boldsymbol{s}'|) p(\hat{\boldsymbol{u}}, \boldsymbol{s} - \boldsymbol{s}') \tag{29}$$

where $k(s)$ is the conventional kernel used in 2D tomography, i.e. the inverse 1D Fourier transform of the ramp filter $|\boldsymbol{\nu}|/2$ (Herman 1980). The usual form of 2D filtered backprojection can be seen by rewriting equations (28) and (29) in a coordinate system with the unit vector $\hat{\boldsymbol{o}}$ along the z axis, $\boldsymbol{x} = (x, y, 0)$, and $\hat{\boldsymbol{u}} = (\cos\theta \sin\phi, \sin\theta \sin\phi, \cos\phi)$. In this system, the integral over $\hat{\boldsymbol{u}}$ reduces to a single integral over θ.

Changing the order of integration over $\hat{\boldsymbol{o}}$, $\hat{\boldsymbol{u}}$ and $\boldsymbol{s}'$ we can now reformulate the reconstruction algorithm, equation (27), as a 3D filtered backprojection (equations (4) and (5)) with

$$\begin{aligned} h(\hat{\boldsymbol{u}}, \boldsymbol{s}) &= \frac{k(|\boldsymbol{s}|)}{\iint_A \mathrm{d}^2\hat{\boldsymbol{o}}\, w(\hat{\boldsymbol{o}})} \iint_A \mathrm{d}^2\hat{\boldsymbol{o}}\, w(\hat{\boldsymbol{o}})\, \delta(\hat{\boldsymbol{o}} \cdot \hat{\boldsymbol{u}})\, \delta(\boldsymbol{s} \cdot \hat{\boldsymbol{o}}) \qquad \hat{\boldsymbol{u}} \cdot \boldsymbol{s} = 0 \\ &= \frac{2k(|\boldsymbol{s}|)}{\iint_A \mathrm{d}^2\hat{\boldsymbol{o}}\, w(\hat{\boldsymbol{o}})} \frac{w(\hat{\boldsymbol{u}} \cdot (\boldsymbol{s}/|\boldsymbol{s}|))}{|\boldsymbol{s}|} \qquad \text{if } (\hat{\boldsymbol{u}} \cdot (\boldsymbol{s}/|\boldsymbol{s}|)) \in A \\ &= 0 \qquad \text{otherwise.} \end{aligned} \tag{30}$$

Taking the 2D Fourier transform of equation (30) yields the filter

$$H(\hat{u}, \nu) = \frac{1}{\iint_A d^2\hat{o}\, w(\hat{o})} \iint_A d^2\hat{o}\, \delta(\hat{o} \cdot \hat{u}) w(\hat{o}) \frac{|\nu - (\nu \cdot \hat{o})\hat{o}|}{2} \qquad \nu \cdot \hat{u} = 0. \tag{31}$$

This filter has been published for a truncated spherical detector (with $w = 1$) by Ra *et al* (1982) and named the TTR kernel. It can be checked that this filter, equation (31), satisfies equation (9). It is not, however, factorisable and consequently does not possess the attractive properties discussed in the previous section. In particular, the operations of filtering and backprojection cannot be commuted, and thus filtering must be performed prior to backprojection. Additionally, within the restricted sense defined in § 3.3, the behaviour of this filter in the presence of noise is suboptimal. However, the TTR kernel (equation (30)) for each projection is zero outside a wedge defined by the set of valid planes, i.e. by A. This unique property has been exploited by Cho *et al* (1983) to derive an extended algorithm (ETTR) which allows the incorporation in the reconstruction of incompletely measured projections. These incomplete projections, which are normally rejected to ensure the shift invariance of the aperture Ω, are incomplete only in regions where the corresponding filter value would, in any case, be zero. While the method introduced by these authors is indeed correct, the presentation led to some confusion and the validity of the ETTR algorithm has recently been questioned (Rogers *et al* 1987). Clarification of the rationale behind the ETTR approach is possible based on the above generalised derivation of the TTR kernel.

In order to reconstruct a density distribution $f(x)$ by 3D filtered backprojection the filtered projection $p^F(\hat{u}, s)$, for each direction $\hat{u}$ which contributes to the backprojection at x, must be evaluated at the point $s = x - (x \cdot \hat{u})\hat{u}$ (equation (4)). In general, the convolution kernel $h(\hat{u}, s)$ for a filter satisfying equation (9) is non-zero for almost all $s \in R^2$. Hence, the value of $p^F(\hat{u}, s)$ at $s = x - (x \cdot \hat{u})\hat{u}$ can be evaluated only if the line integrals $p(\hat{u}, s)$ have been measured for all s, thereby excluding the use of incomplete projections.

The TTR kernel (equation (30)) is zero outside the region in the projection plane defined by the intersection of all valid reconstruction planes. In order to evaluate the convolution of the projection with the kernel at the point $s = x - (x \cdot \hat{u})\hat{u}$ only projection values which lie inside the support of the TTR kernel when centred at s are required. It is not, therefore, necessary that all projections included in the reconstruction are completely measured. For the ETTR algorithm, then, the set of valid planes used to reconstruct the density distribution at x need not be independent of x. A discussion of the practical implementation of this algorithm (Cho *et al* 1983) and of other algorithms allowing a better utilisation of the available data (Defrise *et al* 1987, Clack *et al* 1988) is beyond the scope of this paper.

4.2. Comparison with a factorisable filter

It is interesting to compare the TTR filter (equation (31)) with the factorisable filter (equation (11)) for a truncated cylindrical detector with its axis along the z direction. The corresponding aperture is then

$$\Omega = \{\hat{u} \in S^2 \,|\, |\hat{u}_z| < \sin\theta_0\} \tag{32}$$

and the set of valid planes is given by

$$A = \{\hat{o} \in S^2 \,|\, |\hat{o}_z| > \cos\theta_0\} \tag{33}$$

for some fixed aperture angle θ_0. Evaluation of the expressions in equations (11) and (31) with $w(\hat{\boldsymbol{u}})=1$ then yields the filters derived respectively by Colsher (1980) (H_C) and Ra *et al* (1982) (H_R):

$$
\begin{aligned}
H_C(\boldsymbol{\nu}) &= \frac{|\boldsymbol{\nu}|}{2\pi} && \text{if } \cos\Psi > \cos\theta_0 \\
&= \frac{|\boldsymbol{\nu}|}{4}\,\frac{1}{\sin^{-1}(\sin\theta_0/\sin\Psi)} && \text{if } \cos\Psi < \cos\theta_0
\end{aligned}
\tag{34}
$$

and

$$
\begin{aligned}
H_R(\hat{\boldsymbol{u}},\boldsymbol{\nu}) &= \frac{|\boldsymbol{\nu}|}{2\pi(1-\cos\theta_0)}\left(1-\frac{\cos\theta_0\cos\Psi}{u_p^2}\right) && \text{if } \cos\Psi > \cos\theta_0 \\
&= \frac{|\boldsymbol{\nu}|}{2\pi(1-\cos\theta_0)}\left(1-\frac{\cos^2\theta_0}{u_p^2}\right)^{1/2}\left(1-\frac{\cos^2\Psi}{u_p^2}\right)^{1/2} && \text{if } \cos\Psi < \cos\theta_0
\end{aligned}
\tag{35}
$$

where $u_p^2 = 1-\hat{u}_z^2$ and $\cos\Psi = |\nu_z|/|\boldsymbol{\nu}|$.

The behaviour of these filters H_C and H_R is shown in figure 1 for an aperture $\theta_0 = 50°$. The particular projection shown has $|\hat{u}_z| = 0.50$, and the filters are plotted for $|\boldsymbol{\nu}| = 1$, as a function of ξ, the angle of the frequency vector in the projection plane perpendicular to $\hat{\boldsymbol{u}}$ (i.e. $\nu_z = |\boldsymbol{\nu}|\cos\Psi = u_p \sin\xi$). It is interesting to note the smaller range of the angular part of the factorisable filter; this property can be checked from equations (34) and (35) to be valid for any projection (i.e. any value of $|\hat{u}_z|$) and is consistent with the optimality property discussed above in § 3.3.

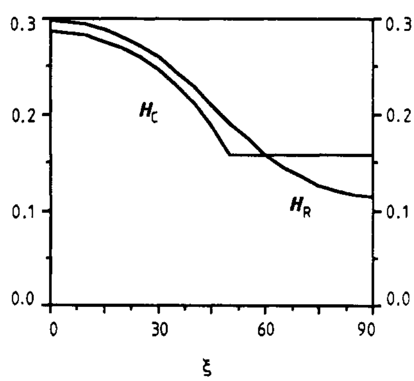

Figure 1. A comparison between a factorisable filter H_C (Colsher 1980) and a non-factorisable filter H_R (Ra *et al* 1982).

4.3. *A general class of filters*

Finally, as a demonstration of the redundancy intrinsic in the 3D data set and of the non-uniqueness of the recovery filter, a class of inversion filters is derived for the truncated cylindrical detector geometry defined by equation (32). The discussion will be restricted to filters $H(\hat{\boldsymbol{u}}, \boldsymbol{\nu})$ with the same cylindrical symmetry as the detector, which means that the filter can be written as $H(\theta, \psi, |\boldsymbol{\nu}|)$, where $\hat{u}_z = \cos\theta$ and $\nu_z = |\boldsymbol{\nu}|\cos\psi$. Then, integration of the Dirac delta function in equation (9) results in

$$\int_{-\min(\sin\theta_0, \sin\Psi)}^{+\min(\sin\theta_0, \sin\Psi)} \mathrm{d}(\cos\theta) \frac{2H(\theta, \Psi, |\boldsymbol{\nu}|)}{|\boldsymbol{\nu}|(\sin^2\Psi - \cos^2\theta)^{1/2}} = 1 \qquad \text{for all } \Psi. \tag{36}$$

A whole class of filters can be constructed using finite Chebyshev series (Fox and Parker 1968)

$$H(\theta, \Psi, |\boldsymbol{\nu}|) = |\boldsymbol{\nu}| \sum_{n=0}^{N} c_n(\Psi) T_n\left(\frac{\cos\theta}{\sin\Psi}\right) \tag{37}$$

where $T_n(\cos\xi) = \cos(n\xi)$ and the number of terms N is arbitrary. The condition for a valid reconstruction filter, equation (36), then becomes

$$\sum_{n=0}^{N} c_n(\psi) r_n(\psi) = 1 \qquad \text{for all } \psi \tag{38}$$

where

$$\int_{-\min(\sin\theta_0, \sin\psi)}^{+\min(\sin\theta_0, \sin\psi)} \mathrm{d}(\cos\theta) \frac{2}{(\sin^2\psi - \cos^2\theta)^{1/2}} T_n\left(\frac{\cos\theta}{\sin\psi}\right) = r_n(\psi). \tag{39}$$

This integral is zero for odd values of n, while for even values of n it is given by

$$\begin{aligned} r_n(\psi) &= 0 && \text{if } \psi < \theta_0 \\ &= -\frac{4}{n}\sin\left[n\cos^{-1}\left(\frac{\sin\theta_0}{\sin\psi}\right)\right] && \text{if } \psi > \theta_0. \end{aligned} \tag{40}$$

Finally, for $n = 0$

$$\begin{aligned} r_0(\psi) &= 2\pi && \text{if } \psi < \theta_0 \\ &= 4\sin^{-1}\left(\frac{\sin\theta_0}{\sin\psi}\right) && \text{if } \psi > \theta_0. \end{aligned} \tag{41}$$

A reconstruction filter can now be constructed by arbitrarily choosing the functions c_n for all $n \geqslant 1$. The first coefficient c_0 is then determined so as to satisfy equation (38), which is always possible since $r_0(\psi) \neq 0$ for all ψ. Colsher's filter H_C, for example, is obtained by taking $c_n(\psi) = 0$ for all $n \geqslant 1$.

5. Conclusions

This paper has explored the relationship between a number of algorithms that have been proposed in recent years for 3D image reconstruction. It has been shown that, as a consequence of the intrinsic redundancy in the 3D data set, each algorithm yields a valid reconstruction, even though the filters used are mathematically distinct. For noise-free data, the reconstructions are identical. It has been seen that all such filters must satisfy a general condition, and two different families of filters—factorisable and non-factorisable—have been studied in detail. It has been shown that factorisable filters have a number of interesting properties, including the possibility to commute the operations of backprojection and filtering. Factorisable filters are seen to have optimal properties in the presence of noisy data.

The second class of filters that were studied are non-factorisable and include the TTR algorithm published by Ra *et al* in 1982. This algorithm, and its extension to the ETTR algorithm (Cho *et al* 1983), has been generalised and the potential of such non-factorisable filters to incorporate incompletely measured projections into the reconstruction has been discussed. Non-factorisable filters, it has been seen, do not share the optimum noise properties of factorisable filters. Recently it has been shown (Defrise *et al* 1987) that algorithms based on factorisable filters can also be modified to incorporate partially measured projection data. However, the efficiency with which these algorithms incorporate incomplete projections, and the noise properties of the reconstructed images, will need further study.

Acknowledgments

MD is Research Associate with the National Fund for Scientific Research (Belgium).

Appendix

We demonstrate here that a non-factorisable filter can be constructed for any non-trivial aperture Ω (i.e. not simply consisting of one great circle on the unit sphere). The reason why this proof is not trivial is that the equation (10) for a factorisable filter needs not be satisfied for all pairs $(\hat{\boldsymbol{u}}, \boldsymbol{\nu})$ but only for the orthogonal pairs $\hat{\boldsymbol{u}} \cdot \boldsymbol{\nu} = 0$. Therefore the fact that the explicit form of a filter $H(\hat{\boldsymbol{u}}, \boldsymbol{\nu})$ does not seem to be factorisable is not a sufficient proof.

Select any three unit vectors $\hat{\boldsymbol{u}}_1, \hat{\boldsymbol{u}}_2, \hat{\boldsymbol{u}}_3$ in Ω not lying on a common equatorial circle. Define as Γ_1 the intersection of the equatorial circle through $\hat{\boldsymbol{u}}_2$ and $\hat{\boldsymbol{u}}_3$ with the acceptance region Ω. Similarly, define Γ_2 and Γ_3. Denote by $\boldsymbol{\nu}_1, \boldsymbol{\nu}_2, \boldsymbol{\nu}_3$ the unit vectors normal to $\Gamma_1, \Gamma_2, \Gamma_3$ respectively. For instance $\Gamma_1 = \{\hat{\boldsymbol{u}} \in \Omega | \hat{\boldsymbol{u}} \cdot \boldsymbol{\nu}_1 = 0\}$. Finally, denote by l_1, l_2, l_3 the length of $\Gamma_1, \Gamma_2, \Gamma_3$, for example

$$l_1 = \iint_{\Omega} \mathrm{d}^2\hat{\boldsymbol{u}}\, \delta(\hat{\boldsymbol{u}} \cdot \boldsymbol{\nu}_1).$$

We now construct two factorisable filters satisfying (10) and (11), using two weight functions defined as follows:

$$\begin{aligned} w_{\mathrm{A}}(\hat{\boldsymbol{u}}) &= 1 \text{ on } \Omega \\ w_{\mathrm{B}}(\hat{\boldsymbol{u}}) &= 1 \text{ on } \Gamma_1 \\ &\quad 2 \text{ in } \hat{\boldsymbol{u}} = \hat{\boldsymbol{u}}_1 \\ &\quad \text{defined along } \Gamma_2 \text{ such that its integral along } \Gamma_2 \text{ is equal to } \xi l_2 \\ &\quad \text{defined along } \Gamma_3 \text{ such that its integral along } \Gamma_3 \text{ is equal to } \rho l_3 \\ &\quad \text{arbitrarily defined elsewhere as a positive integrable function} \end{aligned}$$

where ξ and ρ are two positive numbers with $\xi \neq \rho$. The two factorisable filters are now given by

$$H_{\mathrm{A,B}}(\hat{\boldsymbol{u}}, \boldsymbol{\nu}) = \frac{w_{\mathrm{A,B}}(\hat{\boldsymbol{u}})}{\iint_{\Omega} \mathrm{d}^2\hat{\boldsymbol{u}}'\, \delta(\hat{\boldsymbol{u}}' \cdot \boldsymbol{\nu})\, w_{\mathrm{A,B}}(\hat{\boldsymbol{u}}')}.$$

We now prove that the filter $H=(H_A+H_B)/2$ (which satisfies the general equation (9)) is not factorisable. Indeed, if it were, the ratio

$$R=\frac{H(\hat{\boldsymbol{u}}_1,\boldsymbol{\nu}_2)H(\hat{\boldsymbol{u}}_2,\boldsymbol{\nu}_3)H(\hat{\boldsymbol{u}}_3,\boldsymbol{\nu}_1)}{H(\hat{\boldsymbol{u}}_2,\boldsymbol{\nu}_1)H(\hat{\boldsymbol{u}}_3,\boldsymbol{\nu}_2)H(\hat{\boldsymbol{u}}_1,\boldsymbol{\nu}_3)}$$

would be equal to unity. Note that the ratio R includes only pairs $(\hat{\boldsymbol{u}},\boldsymbol{\nu})$ satisfying $\hat{\boldsymbol{u}}\cdot\boldsymbol{\nu}=0$. We can check that

$$R=\frac{(\xi+2)(\rho+1)}{(\xi+1)(\rho+2)}\neq 1$$

when $\xi\neq\rho$, since, according to the definitions of H_A and H_B, we have

	H_A	H_B
$\hat{\boldsymbol{u}}_1,\boldsymbol{\nu}_2$	$1/l_2$	$2/\xi l_2$
$\hat{\boldsymbol{u}}_1,\boldsymbol{\nu}_3$	$1/l_3$	$2/\rho l_3$
$\hat{\boldsymbol{u}}_2,\boldsymbol{\nu}_3$	$1/l_3$	$1/\rho l_3$
$\hat{\boldsymbol{u}}_2,\boldsymbol{\nu}_1$	$1/l_1$	$1/l_1$
$\hat{\boldsymbol{u}}_3,\boldsymbol{\nu}_1$	$1/l_1$	$1/l_1$
$\hat{\boldsymbol{u}}_3,\boldsymbol{\nu}_2$	$1/l_2$	$1/\xi l_2$.

Therefore it is possible to build at least one non-factorisable filter for any non-trivial aperture.

Résumé

Reconstruction d'images tridimensionnelles à partir de projections globales.

La reconstruction d'images médicales tridimensionnelles en tomographie par transmission et émission est classiquement réduite à un ensemble de reconstructions bidimensionnelles dans des sections transverses parallèles. Il existe cependant un intérêt croissant pour la reconstruction directe des projections en trois dimensions. En tomographie d'émission en particulier, un tel processus de reconstruction rendrait plus efficace l'utilisation du flux de photons utilisable. Dans les dernières années, plusieurs auteurs ont étudié les problèmes associés aux reconstructions tridimensionnelles globales, plus spécialement dans le cas de la tomographie par positrons où la reconstruction tridimensionnelle offre certainement les plus grands avantages. Tandis que la plupart des approches reposent sur la rétroprojection filtrée, la relation entre les différents filtres qui ont été proposés est loin d'être évidente. Ce travail clarifie cette relation par l'analyse et la généralisation des différentes classes de filtres publiées, et établit les propriétés et caractéristiques d'une solution générale du problème de la reconstruction tridimensionnelle. Les auteurs suggèrent quelques règles pour le choix d'un filtre approprié à une situation donnée.

Zusammenfassung

Dreidimensionale Bildrekonstruktion aus vollständigen Projektionen.

Bei der dreidimensionalen medizinischen Bildrekonstruktion sowohl für Transmissionsals auch für Emissionstomographie wurde bisher das Problem in eine Reihe von zweidimensionalen Rekonstruktionen paralleler Querschnitte zerlegt. Es gibt jedoch ein zunehmendes Interesse an der direkten Rekonstruktion der Projektionsdaten in drei Dimensionen. Insbesondere für die Emissionstomographie würde ein solches Rekonstruktionsverfahren den verfügbaren Photonenfluß viel besser nutzen. In den letzten Jahren haben eine Reihe von Autoren die mit einer vollen dreidimensionalen Rekonstruktion verbundenen Probleme untersucht, besonders in der Positronentomographie, wo eine dreidimensionale Rekonstruktion wahrscheinlich den größten Nutzen zu bieten hätte. Während die meisten Ansätze dem gefilterter Rückprojektionen folgen,

sind die Beziehungen zwischen den verschiedenen Filtern die vorgeschlagen wurden bisher nicht bewiesen. Die vorliegende Arbeit untersucht diese Beziehungen durch Analyse und Verallgemeinerung der verschiedenen Arten veröffentlichter Filter und stellt die Eigenschaften und Charakteristiken einer allgemeinen Lösung des dreidimensionalen Rekonstruktionsproblems dar. Einige Richtlinien für die Wahl eines geeigneten Filters für eine gegebene Situation werden vorgeschlagen.

References

Barrett H H and Swindell W 1981 *Radiological Imaging* (New York: Academic Press)

Cho Z H, Ra J B and Hilal S K 1983 True three-dimensional reconstruction—application of algorithm towards full utilization of oblique rays *IEEE Trans. Med. Imaging* **MI-2** 6–18

Chu G and Tam K C 1977 Three-dimensional imaging in the positron camera using Fourier techniques *Phys. Med. Biol.* **22** 245–65

Clack R, Townsend D W and Defrise M 1989 An algorithm for three-dimensional reconstruction incorporating cross-plane rays *IEEE Trans. Med. Imaging* to be published

Colsher J G 1980 Fully three-dimensional positron emission tomography *Phys. Med. Biol.* **25** 103–15

Davison M E 1983 The ill-conditioned nature of the limited angle tomography problem *SIAM J. Appl. Math.* **43** 428–48

Defrise M, Kuijk S and Deconinck F 1987 A new three-dimensional reconstruction method for positron cameras using plane detectors *Phys. Med. Biol.* **33** 43–51

Fox L and Parker I B 1968 *Chebyshev Polynomials in Numerical Analysis* (Oxford: Oxford University Press)

Grangeat P 1987 Analyse d'un système d'imagerie 3D par reconstruction à partir de radiographies X en géométrie coniques *PhD Thesis* Ecole Nationale Supérieure des Télécommunications

Herman G T 1980 *Image Reconstruction from Projections* (New York: Academic Press)

Kinahan P E, Rogers J G, Harrop R and Johnson R R 1987 Three-dimensional image reconstruction in object space *IEEE Trans. Nucl. Sci.* **NS-35** 635–8

Natterer F 1986 *The Mathematics of Computerized Tomography* (New York: Wiley)

Orlov S S 1976 Theory of three-dimensional reconstruction. 1. Conditions of a complete set of projections *Sov. Phys.-Crystallogr.* **20** 312–4

Pelc N J and Chesler D A 1979 Utilization of cross-plane rays for three-dimensional reconstruction by filtered back-projection *J. Comput. Assist. Tomogr.* **3** 385–95

Ra J B, Lim C B, Cho Z H, Hilal S K and Correll J 1982 A true three-dimensional reconstruction algorithm for the spherical positron emission tomograph. *Phys. Med. Biol.* **27** 37–50

Rogers J G, Harrop R and Kinahan P E 1987 The theory of three-dimensional image reconstruction *IEEE Trans. Med. Imaging* **MI-6** 239–43

Schorr B and Townsend D W 1981 Filters for limited-angle tomography *Phys. Med. Biol.* **26** 305–12

Schorr B, Townsend D W and Clack R 1983 A general method of three-dimensional filter computation *Phys. Med. Biol.* **28** 305–12

Smith B D 1985 Image reconstruction from cone-beam projections: Necessary and sufficient conditions and reconstruction methods *IEEE Trans. Med. Imaging* **MI-4** 14–25

Smith P R, Peters T M and Bates R H T 1973 Image reconstruction from a finite number of projections *J. Phys. A: Math. Nucl. Gen.* **6** 361–82

Tam K C and Perez-Mendez V 1981a Tomographical imaging with limited angle input *J. Opt. Soc. Am.* **71** 582–92

—— 1981b Limits to image reconstruction with restricted angular input *IEEE Trans. Nucl. Sci.* **NS-28** 179–81